

**Editor:**

As you can see the reviewers, who wrote two excellent commentaries, are now largely satisfied with your manuscript although reviewer 2 has some fairly minor clarifications they would like to see addressed. Myself I feel the manuscript is quite interesting and laudable for its emphasis on the radiative effects on the environmental conditions affecting convective cloud formation rather than any "indirect effect" on e.g. convective invigoration. A minor suggestion I have is to emphasize this aspect in the title, to make it more clear that it is the **radiative perturbation that is being considered**.

Thank you very much for your positive comments on our manuscript. We also appreciate your thoughts regarding the title. We agree with your suggestion and have changed the title to **“Weakening of Tropical Sea Breeze Convective Systems through Interactions of Aerosol, Radiation, and Soil Moisture”** to better reflect the radiative forcing. We have kept the word “Indirect” in the title too given that we do examine the modulation of some of these processes too.

**Reviewer #2:**

I appreciate the authors’ consideration of my comments and their thorough revisions and responses. Most of my concerns have been addressed, and I just have some minor revisions involving clarifying computations, figures, and discussions to consider below.

The authors would like to thank Reviewer 2 for their additional helpful and constructive suggestions. We have addressed each of their comments below. The reviewer comments are in black font, while the authors’ responses are in red for contrast.

1. I’m not entirely clear on how the maximum sea breeze updraft is being computed. It is within 1 km of the surface front but is it anywhere in the column or is it confined to the low levels where the front is forcing air upward? It seems like this should be confined to the lowest levels to assess the vertical motion directly associated with the sea breeze induced convergence (as opposed to buoyantly induced updrafts) with cloud base vertical wind speed being perhaps most relevant. If that is the case, please state that or explain why the calculation used is appropriate for analyzing the sea breeze induced vertical motion.

In Figures 5i and j, the maximum sea breeze updraft was computed within 1 km of the surface front (either ahead of or behind the front) throughout the depth of the column. The reviewer does, however, make a good point. Following the reviewer’s suggestion, we updated Figure 5g by presenting the maximum updraft velocity assessed within 1 km ahead

of and behind the identified surface-based sea breeze front and below 1 km AGL. Most of the cloud bases fall around 1 km AGL and so this seemed to be appropriate. That said, we also tested a 2 km AGL threshold and the results remained similar.

Please note that the maximum updraft discussed in Section 5.2 is different from that shown in Figures 5g and 5h, in that in Section 5.2 we are looking at the maximum values over the entire land and throughout all vertical levels.

We have added the following sentence to address this concern:

Lines 273–276: We assess the low-level (below 1 km AGL) maximum vertical velocity within  $\pm 1$  km of the surface location of the objectively identified front in order to account for any forward bulging or backward tilting of the frontal boundary in relation to the identified location of the front at the surface, as well as to ensure that the updrafts are primarily driven by the frontal convergence as opposed to the possibility of buoyant forcing.

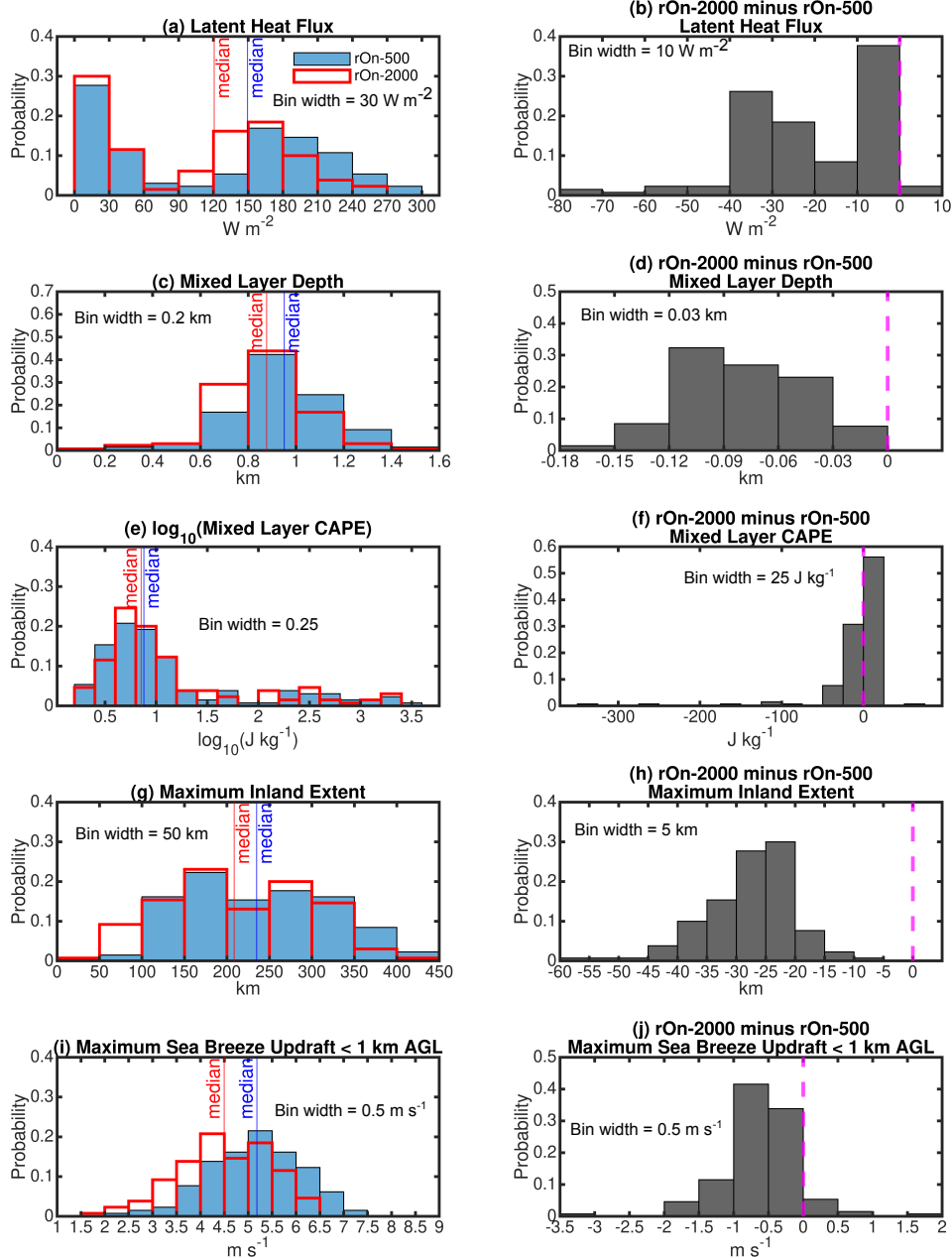


**Figure 5. Histograms of (a) the land-surface latent heat flux ( $W m^{-2}$ ), (c) the surface-based mixed layer depth (km), and (e) the logarithm of the mixed-layer CAPE ( $J kg^{-1}$ ), all of which are averaged for each ensemble from the western domain edge to 50 km ahead of the algorithm-identified sea breeze front between 1200–1800 LT; (g) the maximum inland extent of the sea breeze front (km); and (i) the maximum low-level (below 1 km AGL) updraft velocities within  $\pm 1$  km of the algorithm-identified sea breeze front ( $m s^{-1}$ ). The median values of each characteristic are marked by the red and blue thin vertical lines. The light blue shading and the red lines represent rOn-500 and rOn-2000 ensembles, respectively. Figures (b, d, f, h, and j) are histograms of the differences in the corresponding fields shown in (a, c, e, g, and i) arising due to aerosol loading (rOn-2000 minus rOn-500). The dashed magenta lines indicate where the difference between rOn-2000 and rOn-500 is zero. The bin width of each histogram is marked at the upper corner of each panel.**

2. For Figure 5, the binning can be improved for several panels including e, f, i, and j where most samples are located within only a couple bins. In addition, for the mixed layer CAPE distribution, it would be good to show how many are 0. Similarly, can the bins be made finer in Fig. 6, 7b, and 10 to show more details? I realize there is a limit on the sample size but there is probably a bit more detail that can be communicated. Mean and median differences in the difference panels might also help.

As shown in #1, we have now updated Figure 5e by taking the logarithm of the CAPE values, and we have increased the bin width in Figure 5f. Figures 5i and j were updated by taking the maximum updraft values below 1 km AGL as addressed in comment #1 above. We also changed the bin widths in Figures 6, 7, and 10 to better represent more details of these distributions. We added the following sentence as there is no simulation with averaged CAPE of zero.

Lines 259–260: The minimum CAPE values in rOn-500 and rOn-2000 are 1.8 and 2.0 J kg<sup>-1</sup>.

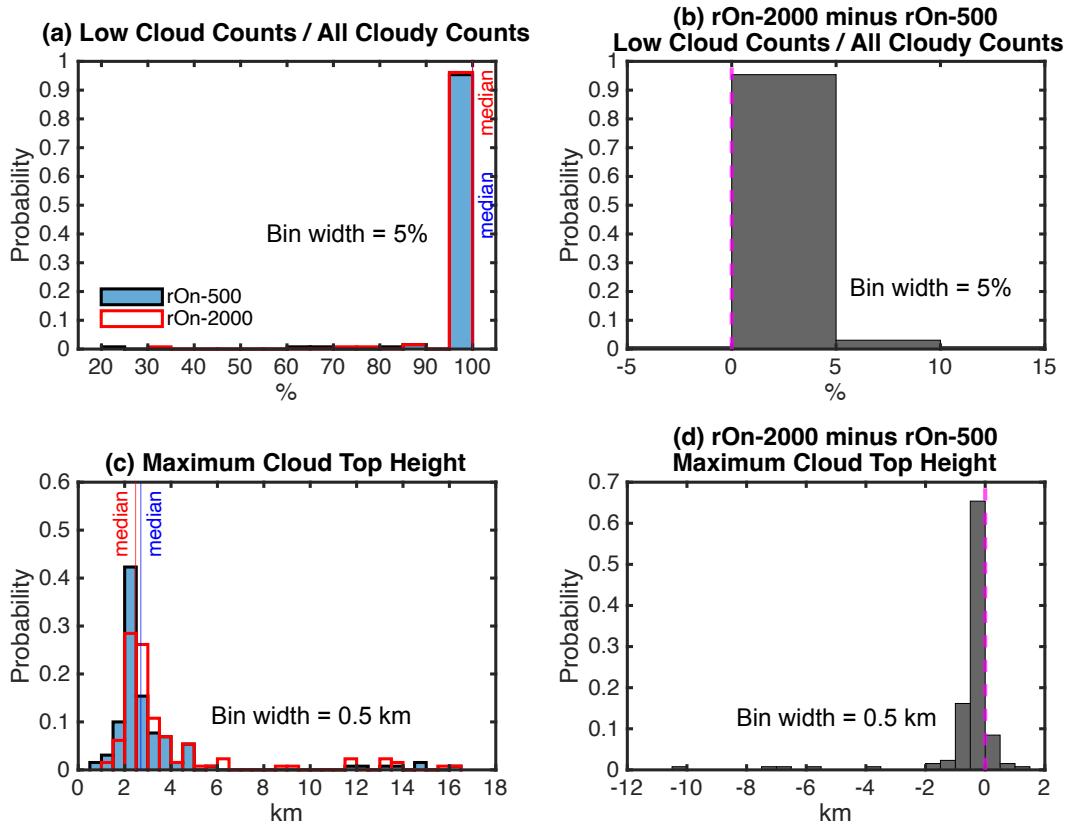


**Figure 6.** Similar to Figure 5 but for histograms of the (a) low cloud (cloud top height < 4 km) fractional contribution to the total number of cloudy columns (low cloud columns / all cloudy columns) and (c) the maximum cloud top height. The right column (b and d) represents rOn-2000 minus rOn-500 difference histograms for the corresponding fields (a and c) in the left column. The dashed magenta lines indicate where the difference between rOn-2000 and rOn-500 is zero. The median values of each characteristic are marked with vertical lines in the left column. The bin width of each histogram is marked at the upper corner of each panel.

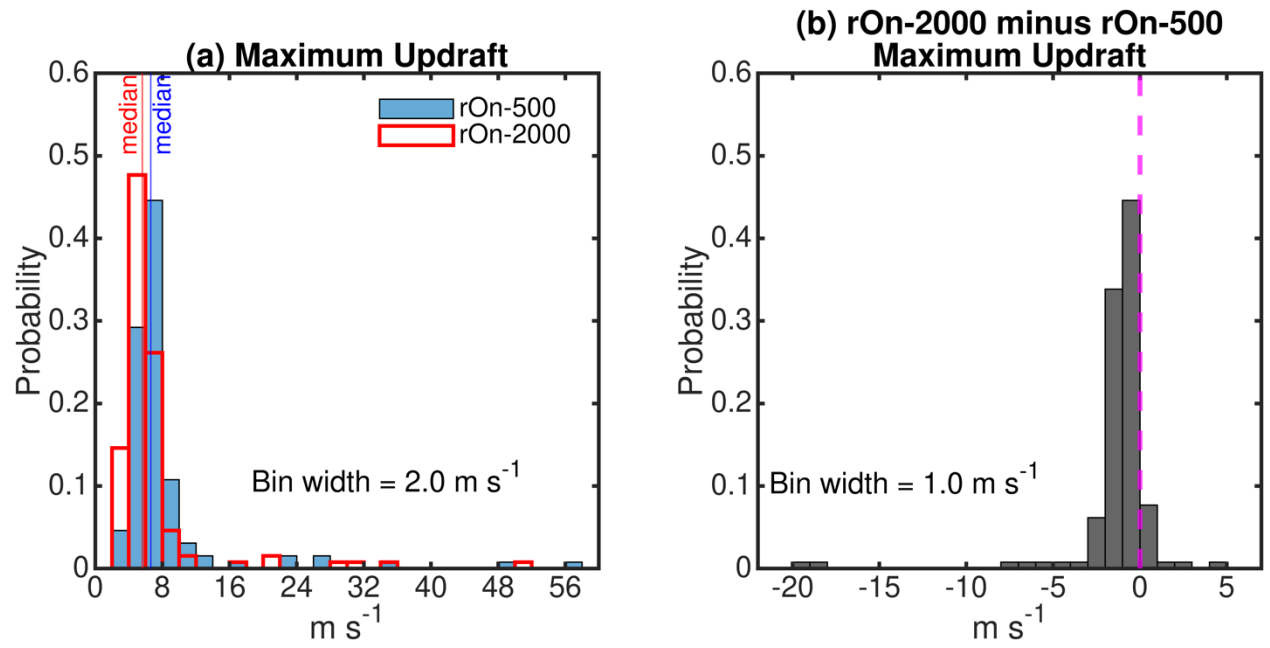


**Figure 7.** Similar to Figure 5 but for (a) histograms of the maximum updraft velocity in rOn-500 and rOn-2000 and (b) a histogram of the maximum updraft velocity differences arising from aerosol loading (rOn-2000 minus rOn-500).

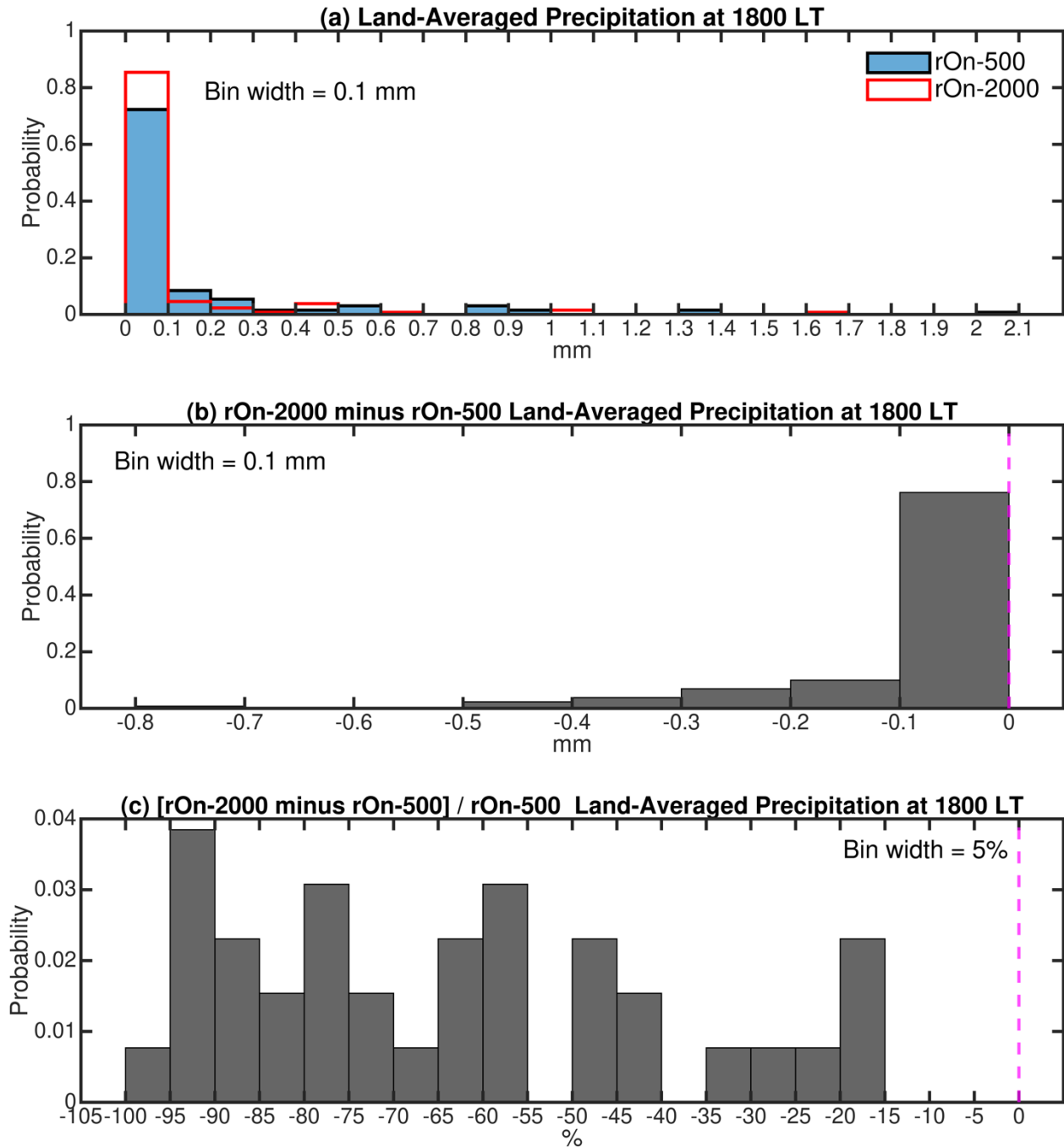


**Figure 10.** A histogram of the land-averaged accumulated surface precipitation at sunset (1800 LT) in rOn-500 (blue) and in rOn-2000 (red) for simulations that produce at least 0.1 mm of the land-averaged accumulated precipitation in rOn-500. The absolute and percent differences between rOn-500 and rOn-2000 are shown in (b) and (c), respectively, where the percentage differences are with respect to rOn-500. The dashed magenta line in (b) and (c) indicates where the difference between rOn-2000 and rOn-500 is zero. The bin width of the histogram is marked on each panel.

- Fig 6c shows a greater median max cloud top height for rOn-500 but the bars would imply something different (i.e., the lowest height bin has many more samples from rOn-500 with the second highest bin shows similar numbers). This must imply that the distribution of values in the second bin (2-4 km heights) is quite different between the 2 runs? If so, I wonder if it makes sense to show more bins so that this is clearer. That would decrease values in the low sample bins, but the peak value would then decrease so you could decrease the y-axis and/or you could also apply non-linear bin widths.

Thank you for this suggestion. We have changed the bin width of Figure 6c to 0.5 km to better present the distribution of cloud top height from 2 to 4 km more clearly, as shown in #2. As the reviewer suspected, this does better demonstrate the link between the median values and the bin distribution.

- Is it appropriate to call all the updrafts “convective”, e.g., in the Section 5.2 title? The sea breeze will certainly force updrafts that are not convecting (i.e., not buoyant). Perhaps these won’t be reflected in the max updraft values being analyzed but that isn’t completely clear either.

Thank you for raising this question. We looked into this further. We now make sure that the maximum updraft velocities are indeed convective (i.e., buoyant) by taking the maximum of the updrafts which are greater than  $1 \text{ m s}^{-1}$  AND have a net positive instantaneous vertical acceleration contribution from the sum of the thermal buoyancy and the condensate loading terms. Adding this constraint on the buoyancy did not qualitatively change the maximum convective updraft results presented in Figures 7 and 8. We updated Figures 7 and 8 to present “convective” updrafts accordingly. We also added the following sentence to the manuscript:

Lines 336–342: To ensure that the maximum updrafts are convective (i.e., positively buoyant) and represent the intensity of sea breeze-initiated convection, we take the maximum updrafts with a net positive instantaneous vertical acceleration contribution from the sum of the thermal buoyancy ( $g \frac{\theta'}{\theta_0} + gr'_v \frac{(1-\varepsilon)}{\varepsilon}$ ) and condensate loading ( $-gr_c$ ) terms in the following vertical momentum equation:  $\frac{\partial w}{\partial t} \approx g \frac{\theta'}{\theta_0} + gr'_v \frac{(1-\varepsilon)}{\varepsilon} - gr_c - \frac{1}{\rho} \frac{\partial p'}{\partial z} - w \frac{\partial w}{\partial z} - u \frac{\partial w}{\partial x} - v \frac{\partial w}{\partial y}$  where  $w$  is vertical velocity,  $g$  is the gravitational acceleration of  $9.8 \text{ m s}^{-2}$ ,  $\theta'$  is the perturbation potential temperature,  $\theta_0$  is the base-state potential temperature,  $r'_v$  is the perturbation water vapor mixing ratio,  $\varepsilon$  is the ratio of dry air to water vapor gas constants,  $r_c$  is the total condensate mixing ratio.



5. In discussing Fig. 8, technically rOn-2000 has peak updrafts  $> 10$  m/s with boundary layer potential temperature  $< 299$  K even though the text states that it doesn't have updrafts  $> 10$  m/s until 299 K. Please clarify this discussion. In addition, it isn't explained why this is the case. There is discussion of a reduction in boundary layer temperature with enhanced aerosol loading but for a given temperature, deep convection initiation is also reduced with enhanced aerosol loading. Is this related to a change in the capping inversion strength or something else?

Thank you for your comment. We clarified Figure 8 by marking the deep convection simulations in black-lined circles. The requirement on deep convective updrafts is that they have cloud top heights greater than 7 km AGL. We also clarified the following sentences.

Lines 363–366: It is clear from this figure that the sea breeze-initiated deep convective mode (maximum cloud top height greater than 7 km) updrafts in rOn-500 occur in all of the ensemble members in which the initial boundary layer potential temperature is 297 K or greater, and in which the mixed layer CAPE is greatest (not shown).

Lines 367–371: For instance, in rOn-500 while 4 of 12 deep convective simulations with the maximum updraft velocity greater than  $10 \text{ m s}^{-1}$  have initial boundary layer potential temperatures between 297 and 299 K (Figure 8a), the only simulations in rOn-2000 with the maximum cloud top height greater than 7 km and the maximum updraft velocity greater than  $10 \text{ m s}^{-1}$  occur for initial boundary layer potential temperature greater than or equal to 299 K (Figure 8b).

Lines 375–378: Also, if we consider those simulations with the same initial boundary layer potential temperatures, the presence of aerosol reduces deep convection initiation. This is due to the fact that aerosol loading leads to less deep convection initiation due to reduced surface temperatures through the scattering of surface downwelling shortwave radiation by aerosol particles.

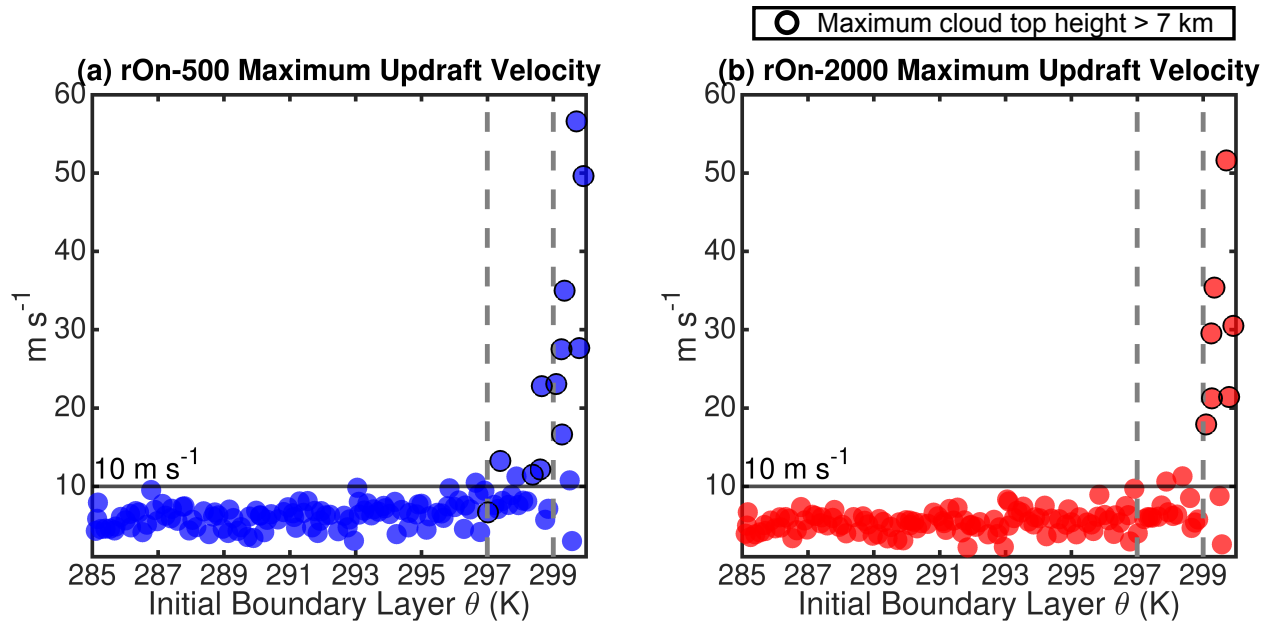


**Figure 8.** Pairwise scatterplots for the maximum updraft velocity ( $\text{m s}^{-1}$ ) versus the initial boundary layer potential temperature (K) for the (a) rOn-500 and (b) rOn-2000 ensembles. The vertical dashed grey lines refer to the potential temperature thresholds described in the text. Simulations with deep convection, identified by the maximum cloud top height  $> 7 \text{ km}$ , are marked with black circles.

6. It could be useful to know what the percentage decrease in precipitation is in addition to the absolute change in Figure 10 since the meaningfulness of the absolute changes is unclear.

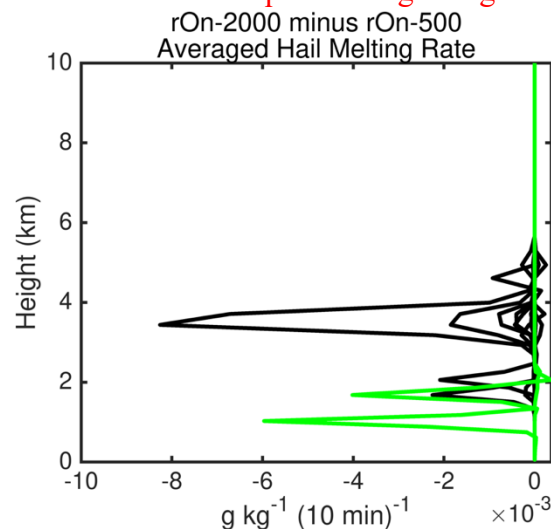
We have updated Figure 10 to include the percentage decrease in precipitation, as shown in #2.

7. In Figure 11, I'm confused by the double peaks in the liquid-ice phase change rates in panels c-e. What is causing the lowest level peaks between 1 and 2 km? Isn't the temperature always well above freezing at these heights? Is this related to hail in some way?

The location of different peaks in Figures 11c–e, particularly for those between 1 and 2 km, are due to different initial conditions. We mentioned this in Lines 467–471. Note that the 1200–1800 LT averaged freezing level ranges from 1.64 to 4.66 km in rOn-500 for the 36 precipitating simulations. In our perturbed parameter ensemble simulations, boundary layer potential temperature ranges from 285 K to 300 K. Depending on other parameter setups in the initial conditions, in some cases, the 0 °C level is located between 1 and 2 km. For example, two of 36 precipitating pairs have a freezing level (averaged over the land domain and during the afternoon) of 1.64 and 2.12 km in rOn-500, respectively. These lower freezing levels are primarily due to their initial boundary layer potential temperature being at the lower end of the range.

Lines 470–472: It should also be noted that the freezing level varies from simulation to simulation due to the different initial temperature and moisture profiles. For example, two of 36 precipitating pairs have a freezing level (averaged over the land domain and during the afternoon) of 1.64 and 2.12 km in rOn-500, respectively. These lower freezing levels are primarily due to their initial boundary layer potential temperature being at the lower end of the range being tested.

The additional figure below shows the rOn-2000 minus rOn-500 melting of hail process rates, averaged over land between 1200 and 1800 LT. The two pairs with a low freezing level are marked with green lines to answer the reviewer's question regarding hail.



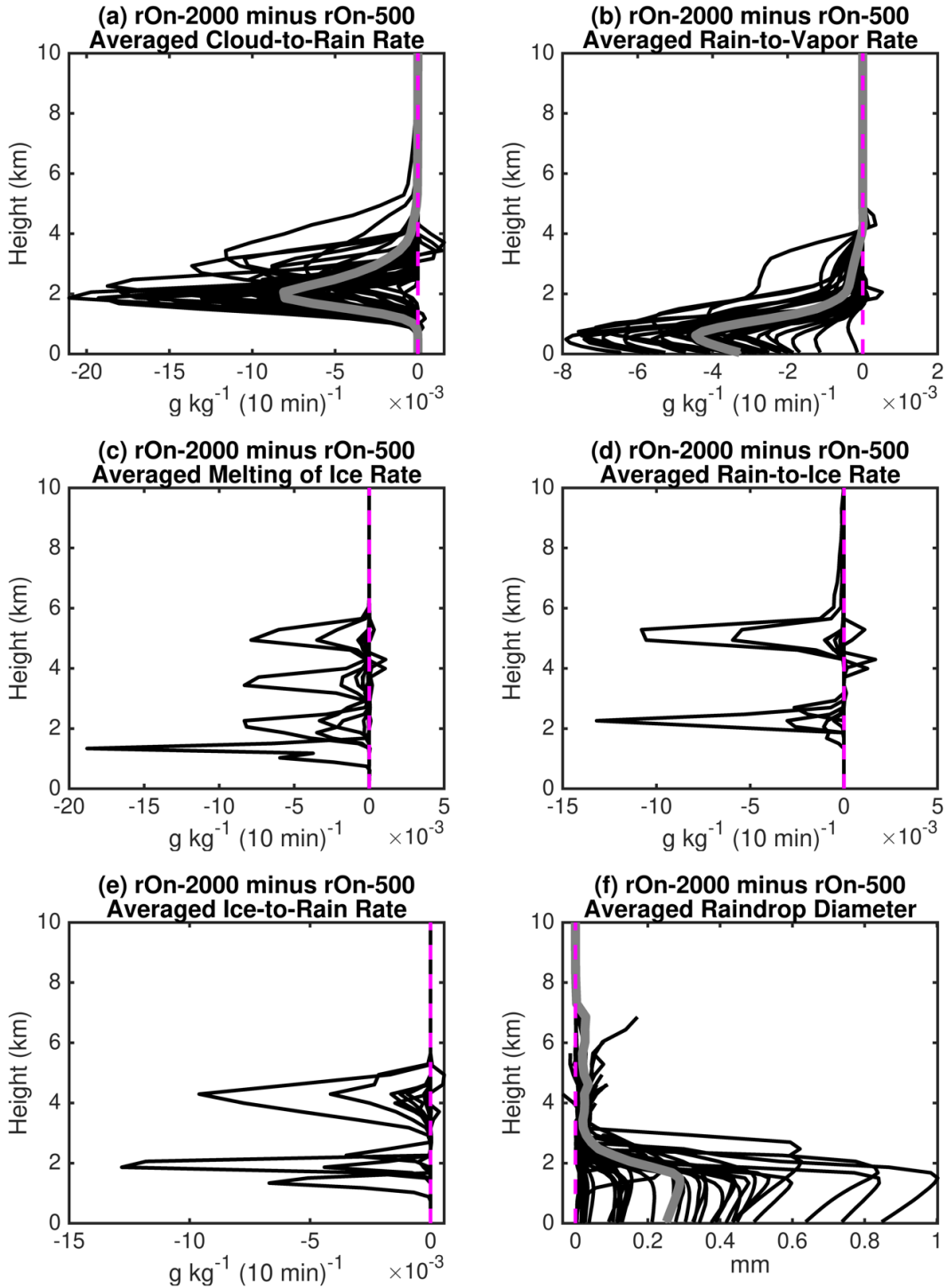


**Figure 11. Aerosol-induced differences to the processes generating rain for the range of environmental conditions tested in these large ensemble experiments. Shown are the rOn-2000 minus rOn500 differences (a) cloud to rain; (b) rain to vapor; (c) melting of ice; (d) rain to ice; and (e) ice to rain rates (see the text for an explanation of these processes) using the 36 ensemble pairs that produce at least 0.1 mm of land-averaged surface accumulated precipitation in rOn-500. Process rates are averaged over the land domain between 1200 and 1800 LT. (f) The rOn-2000 minus rOn-500 raindrop diameter averaged over the land between 1200 and 1800 LT. The thin black lines in all of the figures are from all 36 pairs, and the thick grey lines in a and b are the means of the rOn-2000 minus rOn-500 for the 36 pairs. The dashed magenta lines indicate where the difference between rOn-2000 and rOn-500 is zero.**

8. In the discussion of more evaporation in rOn-500 relative to rOn-2000 in Fig. 11, the reason provided is that there are more numerous smaller raindrops in rOn-500, but these rates are averaged across all domain grid points over land, so how is it known that drop size and number differences are the cause as compared to just more widespread or heavier rain rates (as panel a implies), which would also increase evaporation?

We added a panel in Figure 11, showing the rOn-2000 minus rOn-500 averaged rain drop diameter (Figure 11f). Figure 11f shows a robust increase in raindrop diameter in rOn2000 due to enhanced aerosol loading across 36 pairs of precipitating simulations, supporting lines 474–477.

Lines 474–477: Similarly, average rain evaporation rates (i.e., rain-to-vapor) shown in Figure 11b are also greater in magnitude in rOn-500 than rOn-2000, demonstrating that the population of less numerous but larger raindrops formed in rOn-2000 (Figure 11f) evaporate less readily. The production of populations of fewer but larger raindrops in polluted conditions has been observed previously (e.g., Altartz et al. 2007; Storer and van den Heever 2013).

9. Line 490, “loading, that surface” should be “loading, the surface”.

Done.